International Congress Motor Vehicles & Motors 2012

Kragujevac, October 3rd-5th, 2012

MVM2012-026

Marko Kitanović[1]
Slobodan J. Popović[2]
Nenad Miljić[3]
Miroljub Tomić[4]
Predrag Mrđa[5]

A SIMULATION STUDY OF THE EFFECTS OF TURBO-EXPANSION CONCEPT IMPLEMENTATION ON COMBUSTION AND GAS-EXCHANGE PROCESSES OF A 1,4 L SPARK-IGNITION ENGINE

ABSTRACT: Internal combustion engines account for approximately a quarter of global energy demand. The primary reason is the very high reliance of the transportation sector on fossil fuels. Reducing IC Engines' environmental impact and fuel consumption is one of the directions taken by vast research efforts aimed at increasing the sustainability of the transportation sector. One of the possibilities is the use of a charge-air cooling process - turbo-expansion, to raise efficiency by harnessing more exhaust energy and raising the intake charge density. It allows intake-air temperature to be lowered to around, or even below, ambient levels and exempts the turbocharger system from using a wastegate. A co-simulation in WAVE and MATLAB/Simulink environments was conducted to investigate the effects of the turbo-expansion concept on gas-exchange and combustion processes of a small, 1,4 L spark-ignition turbocharged engine. An empirical, operating conditions-correlated, Wiebe-based spark-ignition combustion model was used to predict the influence of intake and exhaust conditions on combustion duration and heat release dynamics. The implications on the engine gas-exchange processes are quantified. Despite significant intake charge cooling effect not being conveyed inside the cylinders, the brake specific fuel consumption is predicted to be reduced by 1,8 % at 4500 RPM.

KEYWORDS: turbo-expansion, internal combustion engine, combustion, gas-exchange, simulation

INTRODUCTION

Despite growing efforts being concentrated on hybrid powertrain technologies, which bring significant fuel consumption reductions, continuing attempts are being made by the research community to raise the overall thermal efficiency of the internal combustion engine. One of the main reasons is the very high reliance of the transportation sector on fossil fuels which, together with its environmental aspects, call for attaining even the smallest of efficiency improvements.

[1] *Marko Kitanović, Research Assistant, Internal Combustion Engines Department, Faculty of Mechanical Engineering, University of Belgrade, Kraljice Marije 16, 11120 Belgrade 35, Serbia, mkitanovic@mas.bg.ac.rs*
[2] *Slobodan J. Popović, Research and Teaching Assistant, spopovic@mas.bg.ac.rs*
[3] *Nenad Miljić, Research and Teaching Assistant, nmiljic@mas.bg.ac.rs*
[4] *Miroljub Tomić, Head of Department, mtomic@mas.bg.ac.rs*
[5] *Predrag Mrđa, Research Assistant, pmrdja@mas.bg.ac.rs*

One of the directions in that regard is exhaust energy recuperation. In conventional SI turbocharged engines, part of the exhaust enthalpy is used to drive a compressor to raise the intake charge density, specific power and with it the mechanical efficiency of the powertrain. Problems arising due to knock phenomenon appearance mean that significant brake thermal efficiency improvements of such downsized SI engines are limited.

Turbo-cooling concept

The propensity for knock to occur is dependent on unburned gas state (temperature and pressure) during flame propagation process, the time available for the unburned charge to complete initial chain reactions leading to spontaneous combustion (engine speed related) and on fuel's intrinsic chain reaction dynamics. One of the possibilities for eliminating knock without sacrificing performance is to supply the engine with lower temperature intake charge for a given density that will result in approximately the same potential brake mean effective pressure without the devastating consequences knock has on combustion chamber elements.

A charge-air intake conditioner system, shown in Figure 1 has been proposed [7] to fulfill the aforementioned needs.

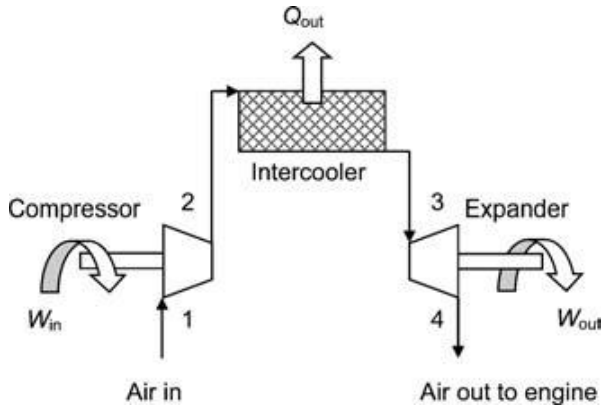

Figure 1 Charge-air conditioner (CAC) system [5]

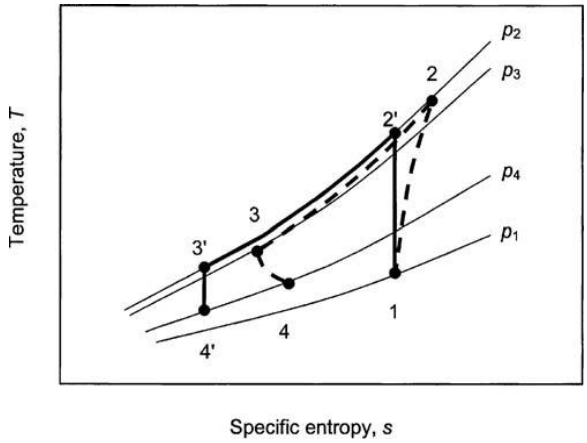

Figure 2 T-s diagram for the CAC process [5]

Air enters the compressor at (1) and exits at (2) with higher specific energy due to energy transfer. Significant temperature drop occurs in the intercooler (2-3), after which air is finally brought to the desired engine intake conditions in the expander, in which pressure and temperature are lowered while expansion work at the shaft is obtained. This system allows air to be cooled to below-ambient temperature, which is not achievable by the intercooler solely.

Several arrangements regarding the implementation of this charge-air cooling system into IC Engine's configuration are available. One of them, which is thoroughly analyzed in [5, 6], involves the use of engine crankshaft power for driving the system. It is also possible to use the power from the exhaust turbine to provide the additional power necessary for CAC operation. In that case, the variable geometry turbine receives the complete flow of exhaust gases and is exempted from using a wastegate valve because the desired intake conditions are regulated by the turbo-expander situated after the intercooler.

Simulation study objectives

In this paper, a comprehensive simulation analysis is performed on an exhaust-gas-driven, charge-air conditioner system-equipped (later referred as turbo-expansion), turbocharged SI IC Engine model. For isolating the potential benefits of the turbo-expansion concept on an SI engine, a baseline model incorporating a variable-geometry turbocharger (VGT), capable of regulating the engine volumetric efficiency without the use of a wastegate, was constructed to serve as the basis for comparison.

By using a predictive, Wiebe-based combustion model, the implications of the turbo-expander on the engine work cycle and in particular the combustion process is analyzed. Because of increased compressor power needs compared to a VGT-equipped IC Engine, the exhaust back-pressure increases and thus induces deterioration in engine charging processes, which need to be offset by gains in knock-free combustion and the additional expansion work benefits for this concept to be effective.

SIMULATION MODEL DESCRIPTION

For evaluating the potential benefits of this concept, a baseline engine model was built in Ricardo WAVE, a 1D engine and gas dynamics simulation software package. A second model, practically representing the baseline model with an additional turbine on the intake side, was also constructed to represent the turbo-expansion equipped powertrain. 1D fluid dynamics equations are solved in intake, exhaust ducts and junctions and a zero-dimensional, two-zone, conservation of energy formulation (the first law of thermodynamics) is applied to the cylinder volume. For implementing the combustion model from Lindstrom et al. [3], a Simulink interface was used to effectively build a co-simulation between the WAVE environment and combustion and knock controllers conceived in Simulink.

Engine models

The turbo-expansion engine model is shown in Figure 3.

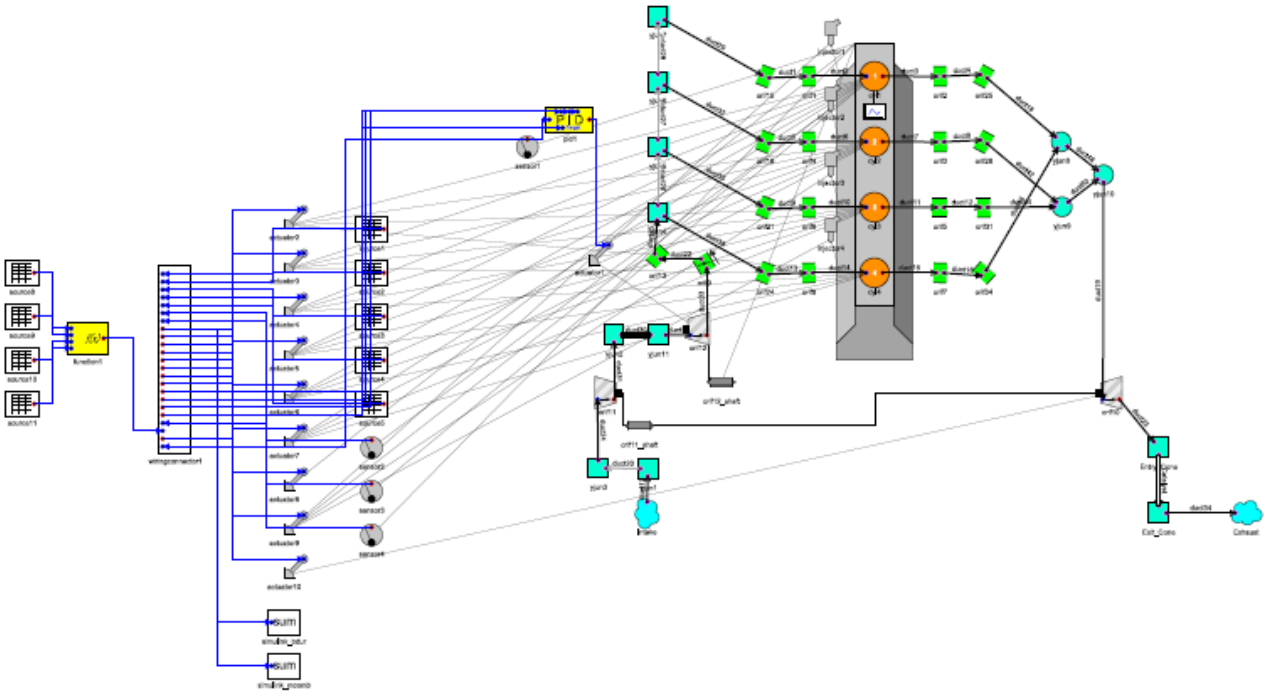

Figure 3 Turbo-expansion engine model

As can be seen, the engine is fitted with an exhaust turbine that supplies power to the compressor. After the compressed air exits the compressor, it enters the intercooler in which significant heat rejection occurs. It should be noted that the effectiveness of the intercooler is held at a constant value of 0,7 across all operating points, both engine models included. The turbo-expander is positioned after the intercooler and is responsible for delivering the engine with desired charge state. The differences between this and the baseline engine model are only related to the turbo-expander being replaced by an orifice with diameter equal to adjoining ducts.

The base engine specifications are presented in Table 1.

Table 1 Engine specifications

Engine configuration	4-cylinder, inline, 8 valves, turbocharged
Bore	80,5 mm
Stroke	67,4 mm
Compression ratio	9,03
Connecting rod length	128,5 mm
Intake Valve Opens	6 CA BTDC
Intake Valve Closes	46 CA ABDC
Exhaust Valve Opens	47 CA BBDC
Exhaust Valve Closes	7 CA ATDC

In both cases, the original Woschni heat transfer model (without the load compensating term) was used to predict the instantaneous heat transfer coefficient in the combustion chamber. For predicting the combustion chamber temperatures needed for heat transfer calculations, the Atkins-French model for petrol engine thermal loading determination was written in MATLAB. The temperatures of the cylinder head (intake and exhaust valves included),

cylinder liner and that of piston top are calculated based on current operating parameters, such as the fuel mass flow, equivalence ratio and engine speed.

Turbomachinery models

For modeling the energy transfer processes in turbomachinery, WAVE “mapless” compressor and turbines are used. The mapless turbine is modeled as a simple nozzle, with mass flow determined by the following equation:

$$\dot{m} = \frac{\pi}{4} D_{eff}^2 \frac{P_{0i}}{\sqrt{RT_{0i}}} \Pi_{ts}^{-1/\kappa} \sqrt{\left[\frac{2\kappa}{\kappa-1}\left(1-\Pi_{ts}^{((1-\kappa)/\kappa)}\right)\right]} \tag{1}$$

where: D_{eff} is the nozzle effective throat diameter

P_{0i} is the stagnation inlet pressure

T_{0i} is the stagnation inlet temperature

Π_{ts} is the total-to-static pressure ratio.

Because turbines typically choke at a pressure ratio higher than the critical pressure ratio of the considered gas, the mass flow-pressure ratio curve of the turbine is stretched to match the critical pressure ratio of the modeled turbine, which is 4 in this case.

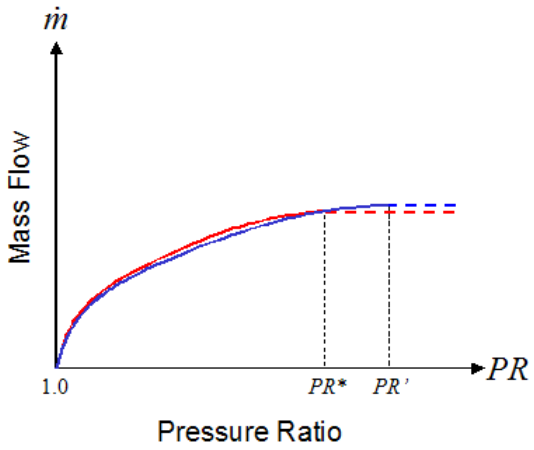

Figure 4 Mapless turbine mass flow-pressure ratio curve [4]

The power produced by the turbine is calculated using the following equation:

$$P = \dot{m} c_p T_{ti} \left(1-\Pi^{((1-\kappa)/\kappa)}\right)\eta_t \tag{2}$$

where: c_p is the specific heat of the gas

T_{ti} is the turbine inlet temperature of the gas

η_t is the turbine isentropic efficiency.

The mapless compressor is modeled in WAVE as a planar rotor and an exit duct, representing a diffuser. Based on the cycle-averaged work obtained from the turbine model, the pressure ratio across the mapless compressor is calculated using the equation for compression power:

$$P = \dot{m} c_p T_{ci} \left(\Pi^{((1-\kappa)/\kappa)} - 1\right)\frac{1}{\eta_c} \tag{3}$$

where: T_{ci} is the compressor inlet temperature of the gas

η_c is the compressor isentropic efficiency.

The exhaust turbine nozzle diameter of the baseline engine is PID controlled to reach a desired volumetric efficiency condition, whereas the turbo-expander is charged with this task in the turbo-expansion engine, as the exhaust turbine nozzle diameter is swept from 26 through 22 to finally 18 mm. Crankshaft power is supplemented by power obtained by gas expansion in the turbo-expander and all brake parameters take into account this additional power (Brake Mean Effective Pressure, Brake Specific Fuel Consumption, brake engine power,...).

Table 2 Turbomachinery models specifications

Exhaust turbine nozzle diameter (turbo-expansion engine)	26, 22, 18 mm sweep
Exhaust turbine isentropic efficiency	0,7
Exhaust turbine choking pressure	4
Compressor isentropic efficiency	0,7
Maximum compressor pressure ratio	4
Turbo-expander isentropic efficiency	0,7
Turbo-expander choking pressure	4

Combustion model

For the purpose of analyzing the effects of turbo-expansion induced changes on gas exchange process and its consequences on combustion, an empirical, predictive, Wiebe-based combustion model from Lindstrom [3] is used. The total burn duration is defined as

$$\Delta\theta = \Delta\theta_0 \cdot g_{SL} \cdot g_{\varphi,spark} \cdot g_n = \Delta\theta_0 \cdot \frac{G_{SL}}{G_{SL,0}} \cdot \frac{G_{\varphi,spark}}{G_{\varphi,spark,0}} \cdot \frac{G_n}{G_{n,0}} \tag{4}$$

where $\Delta\theta_0$ is the reference total burn duration in CAD

g_{SL} is the relative influence of laminar burn velocity

$g_{\varphi,spark}$ is the relative influence of spark timing

g_n is the relative influence of engine speed.

The equation for laminar flame velocity correction is

$$G_{SL} = \frac{1}{S_L\left(\lambda, T_{spark}, p_{spark}, x_{rg}\right)} \tag{5}$$

$$S_L = S_{L,0}\left(\frac{T}{298}\right)^{\alpha_{g,opt}}\left(\frac{p}{1.013}\right)^{\beta_{g,opt}}\left(1-2.06x_{rg}^{0.77}\right) \tag{6}$$

$$S_{L,0} = 30.5 - 54.9\left(\phi - 1.21\right)^2$$

with fuel specific constants for gasoline: $\alpha_{g,opt} = 1.3 - 0.271\phi^{3.51}$

$$\beta_{g,opt} = -0.15 + 0.141\phi^{2.77}.$$

Furthermore, spark timing, with its turbulence-related and ignition delay effects on combustion duration, is also accounted for with the following expression:

$$G_{\varphi,spark} = 1.60 - 0.053\varphi_{spark} + 9.1\cdot 10^{-4}\varphi_{spark}^2. \tag{7}$$

If spark would to occur later than reference timing, combustion duration would tend to increase because of reduced turbulence, which has a peak value near top dead center. On the other hand, ignition delay time would abbreviate because of increased in-cylinder temperature. A third relation, taking into account the correlation of engine speed on total combustion duration is also introduced:

$$G_n = 2.13 - \frac{55.5}{\sqrt{n}}. \tag{8}$$

The combustion mode parameter is defined through combustion duration and engine speed with

$$m = m_0 \cdot \frac{H_{\Delta\theta,n}}{H_{\Delta\theta,n,0}} \tag{9}$$

where $H_{\Delta\theta,n} = -0.0421 \cdot \Delta\theta + 3.51 \cdot 10^{-4} \cdot n + 5.71$.

It should be noted that all of these correlations were identified by analyzing combustion duration and mode parameters of a 4-cylinder, turbocharged, 2 liter, spark-ignition engine. As it can be seen, the total burn duration, along with the combustion mode parameter, is calculated with respect to reference combustion parameters (Table 3).

Table 3 Reference combustion parameters

Engine speed	n=2500 RPM
Spark timing	φ_{spark}=14,9 CAD BTDC
Cylinder temperature @ spark event	T_{spark}=697 K
Excess air ratio, equivalence ratio	λ=1, φ=1
Cylinder pressure @ spark event	p_{spark}=21,5 bar
Residual gas molar fraction	x_{rg}=3,3 %
Combustion mode parameter	m_0=3,97
Total burn duration	$\Delta\theta$=59,9 CAD

The mass fraction burnt relation used throughout this simulation study is the well-known Wiebe equation:

$$x_b(\theta) = 1 - \exp\left[-6.90 \left(\frac{\theta - \theta_0}{\Delta\theta} \right)^{m+1} \right]. \tag{10}$$

Engine knock model

Engine knock is modeled using the Douaud-Eyzat [2] relation for induction time

$$\tau = 0.01869 / A_p \cdot \left(\frac{ON}{100} \right)^{3.4107} \cdot p^{-1.7} \cdot \exp\left(\frac{3800 / A_T}{T} \right) \tag{11}$$

where $ON = 95$ is the octane number of the considered fuel

A_p is the pre-exponential multiplier

A_T is the activation temperature multiplier.

Engine knock occurs when

$$\int \frac{d\tau}{\tau} = 1 \tag{12}$$

during end-gas compression.

The multipliers in equation (11) were both calibrated to 0,95 to account for the knock onset at the reference combustion operating point.

An engine knock controller was built in Simulink to keep engine knock intensity, defined as the mass fraction of unburned charge during knock occurrence, below 0,5 %. It directly controls the start of combustion, advancing spark timing when no knock occurs and retarding it when knock intensity crosses 0,5 %.

The Simulink model that drives the WAVE engine model, supply combustion parameters, chamber elements' temperatures and engine operating conditions is shown in Figure 5.

Engine friction model

For calculating the brake engine parameters, a modified version of the Chen-Flynn friction correlation model was used. The Friction Mean Effective Pressure is defined as:

$$FMEP = ACF + \frac{1}{n_{cyl}} \sum_{i=1}^{ncyl} \left[BCF \cdot P_{\max,i} + CCF \cdot \frac{S \cdot n}{2} + QCF \cdot \left(\frac{S \cdot n}{2} \right)^2 \right] \tag{13}$$

where $ACF = 0.5$ bar - constant portion of the Chen-Flynn friction correlation

$BCF = 0.006$ - term which varies linearly with peak cylinder pressure $P_{\max}$

$CCF = 600 \ \frac{\text{Pa} \cdot \text{min}}{\text{m}}$ - term which varies linearly with piston speed $\frac{S \cdot n}{2}$

$QCF = 0.2 \ \frac{\text{Pa} \cdot \text{min}}{\text{m}}$ - term which varies quadratically with piston speed $\frac{S \cdot n}{2}$

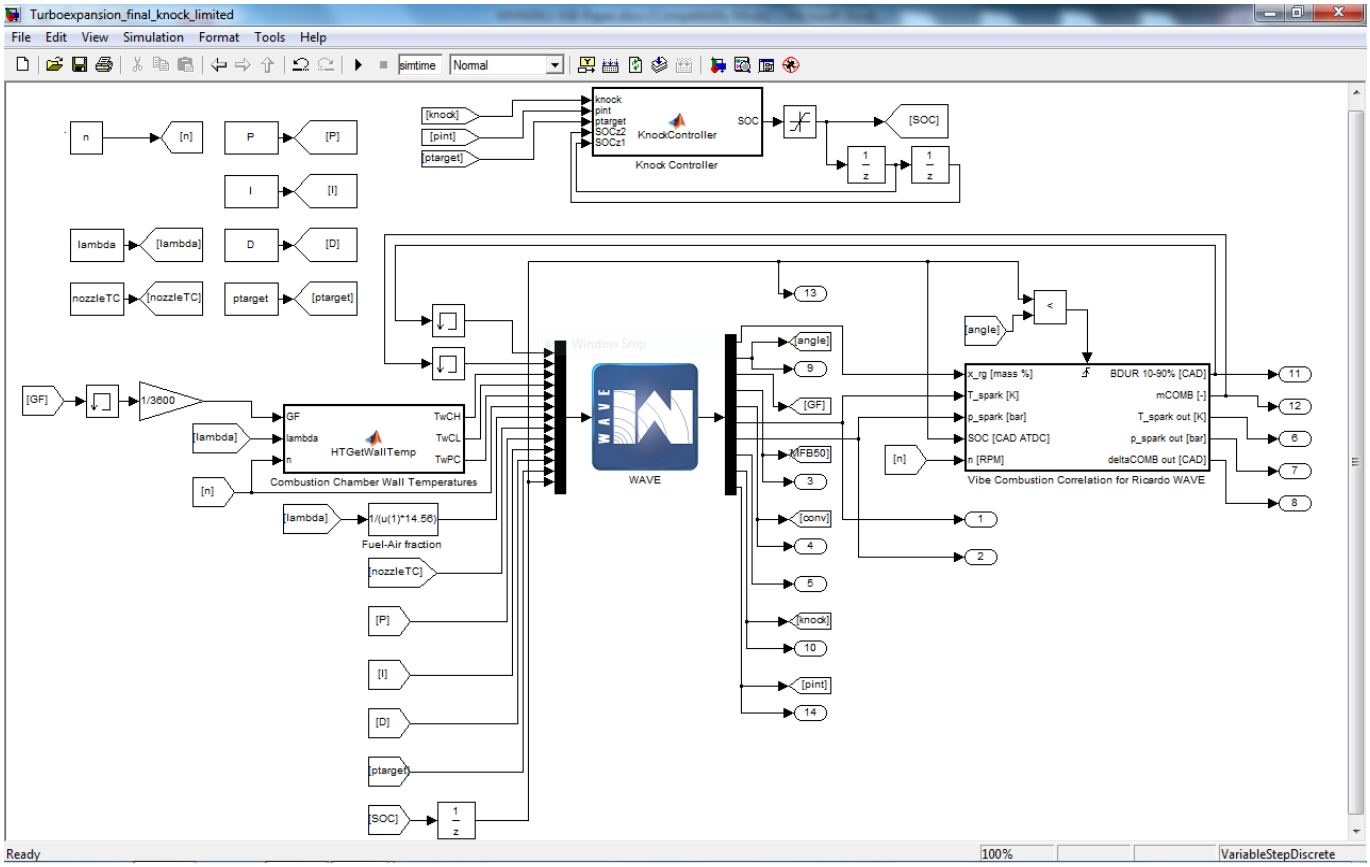

Figure 5 Main Simulink model

RESULTS

The engine volumetric efficiency was regulated by means of a PID controller on both engine models, throughout the entire engine speed operating range. The volumetric efficiency parameter is defined as

$$\frac{m_{air,in}}{V_d \cdot \rho_{std}} = 1{,}4 \tag{14}$$

Where V_d is the engine displacement and ρ_{std} is the air density at standard conditions (298 K, 1 bar). It should be noted that this simulation study was conducted at full throttle only and with lambda value of 1.

The in-cylinder pressure data for the 13 baseline engine cycles (corresponding to converged cycles for engine speed range of 2000-5000 RPM in 13 steps) and the 39 turbo-expansion (TE) engine cycles (13 engine speeds sweep times 3 exhaust turbine nozzle effective diameter values) are shown in Figure 6 and 7. The large difference

in pressure (Figure 8) and temperature (Figure 9) at Intake Valve Closing (IVC) event in the range of 2500 – 3500 RPM is indirectly due to a large difference in charging efficiency between the two engine models, introduced by adding a turbine on the intake side of the engine. The presence of the turbo-expander changes the pressure waves' amplitude and propagation characteristics. Even though the volumetric efficiency for all the operating regimes is the same (equal to 1,4), the cycle-averaged pressure in intake runners is lower due to charging efficiency spike (Figure 10).

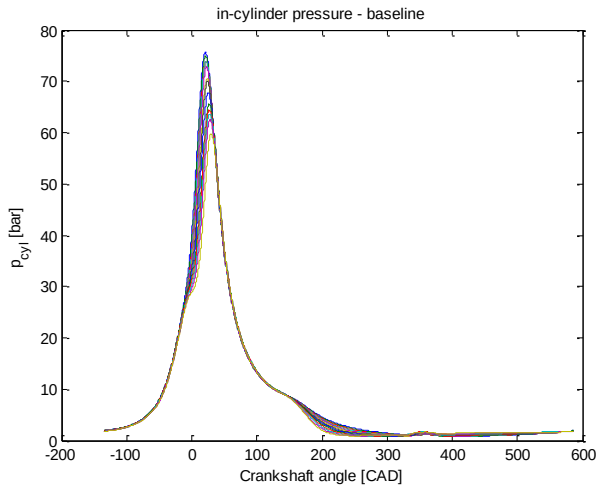

Figure 6 In-cylinder pressure for baseline turbocharged engine model

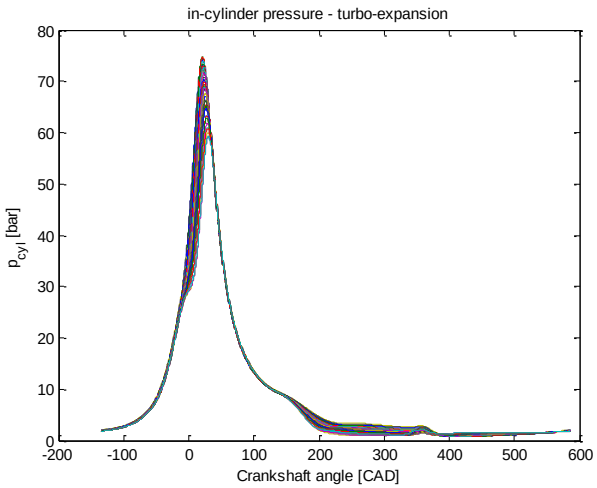

Figure 7 In-cylinder pressure for turbo-expansion engine model

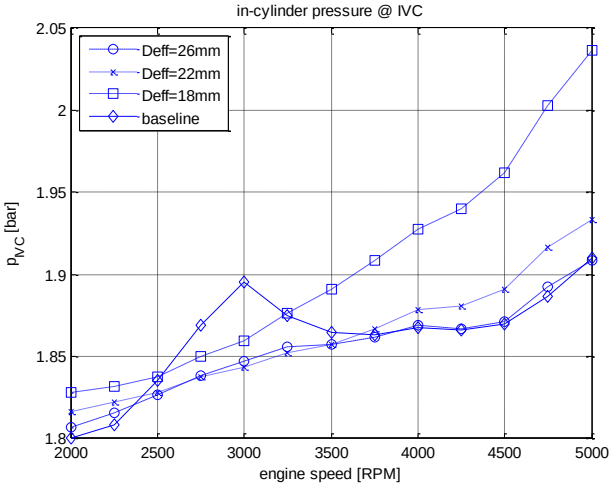

Figure 8 In-cylinder pressure @ IVC

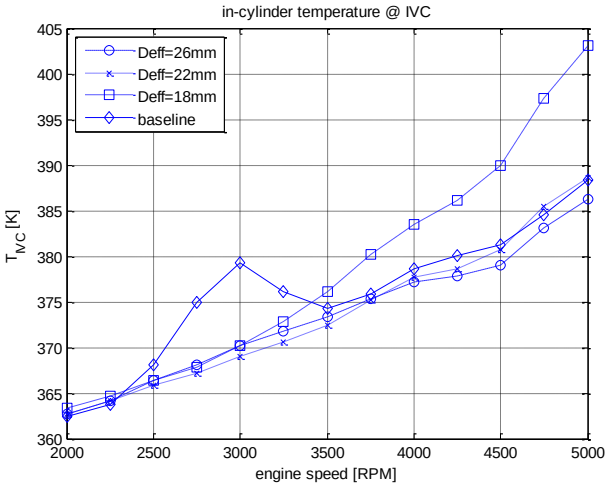

Figure 9 In-cylinder temperature @ IVC

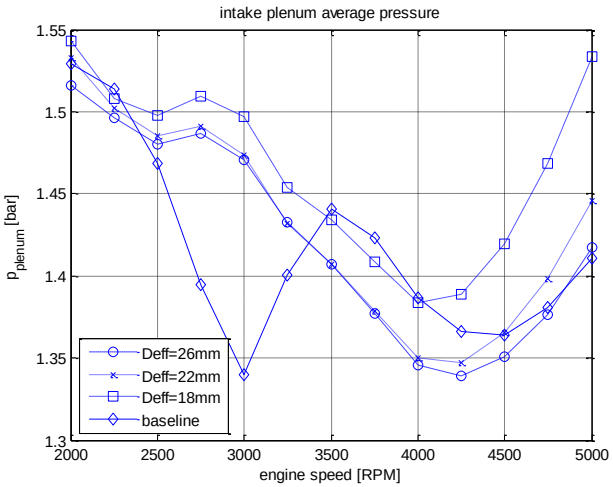

Figure 10 Time-averaged intake plenum pressure

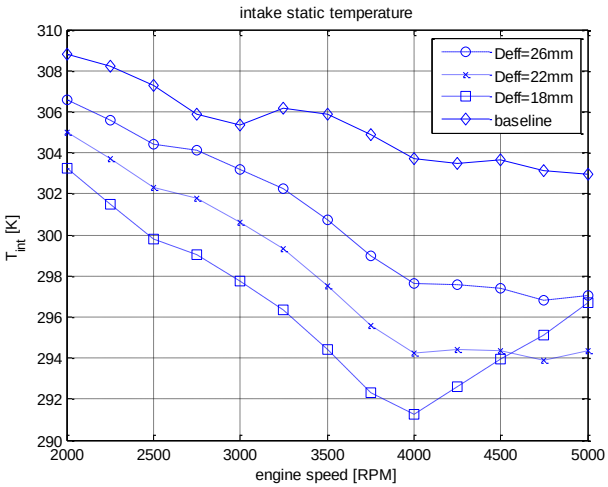

Figure 11 Mass-flow averaged intake static temperature

This has the effect of intensively heating the intake charge by several means (higher backflow, heat transfer from intake valve at greater velocity), leading to an increase in charge temperature and pressure at the start of

compression for the given mass of fuel/air mixture in the baseline engine model. This heating affects engine indicated and effective parameters because of the greater propensity for knock to occur. The knock controller has to retard spark timing to limit knock intensity to values below 0,5 %. This even further intensifies intake charge heating due to increased residual gas temperature in the cylinder.

The mass-flow averaged intake static temperature (Figure 11) drops by increasing the turbo-expansion effect (by reducing the exhaust turbine effective diameter) and the difference between the two engine models reaches 12 °C at 4000 RPM. However, this significant cooling effect is not conveyed inside the cylinder due to increased residual gas mass fraction present in the turbo-expansion engine. The rise in temperature above 4000 RPM occurring on the TE engine model with the smallest exhaust turbine effective diameter (18 mm) is a result of compressor pressure ratio exceeding the maximum value of 4, after which a significant drop in isentropic efficiency occurs.

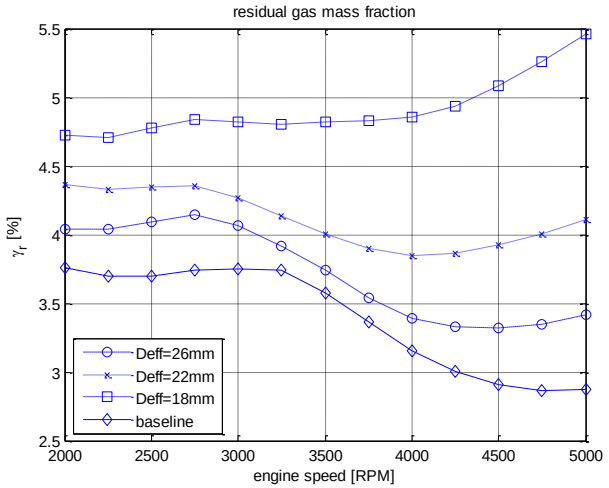

Figure 12 Residual gas mass fraction

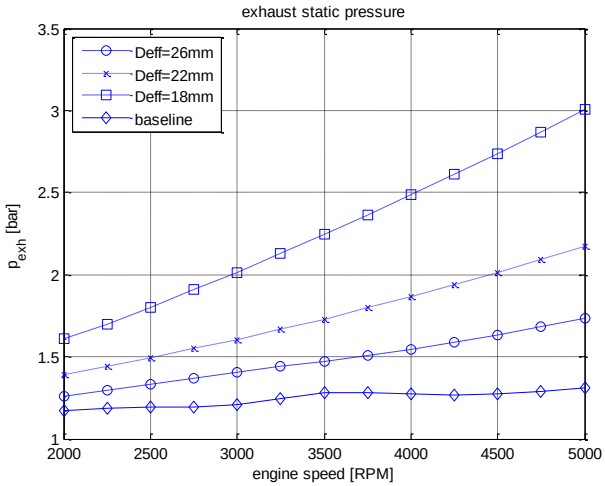

Figure 13 Time-averaged exhaust static pressure

By analyzing the Pumping Mean Effective Pressure (PMEP, Figure 14) and exhaust pressure data (Figure 13), it can be concluded that the addition of the turbo-expander has a significant effect on gas-exchange processes. The time-averaged exhaust static pressure rises by a factor of in excess of 2 in the worst case. The power necessary for driving the intake charge conditioner dictates the increase in exhaust flow restriction at the same mass flow of fresh intake charge through the engine. The PMEP (Figure 14, negative values correspond to negative pumping work) is positive from 2000 RPM to 2750 RPM in the best cases (baseline and TE with *Deff*=26 mm). The detrimental effects on gas-exchange process is partly offset by a greater Gross Indicated Mean Effective Pressure (GMEP), taking into account only the compression and expansion strokes of the cycle. Indeed, the turbo-expansion engine models, precisely the two models with the largest exhaust turbine, have a higher GMEP value throughout engine speeds of 2500 to 4500 RPM.

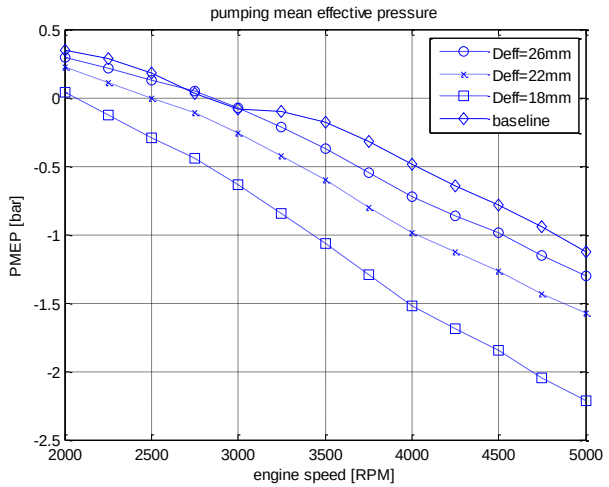

Figure 14 Pumping mean effective pressure

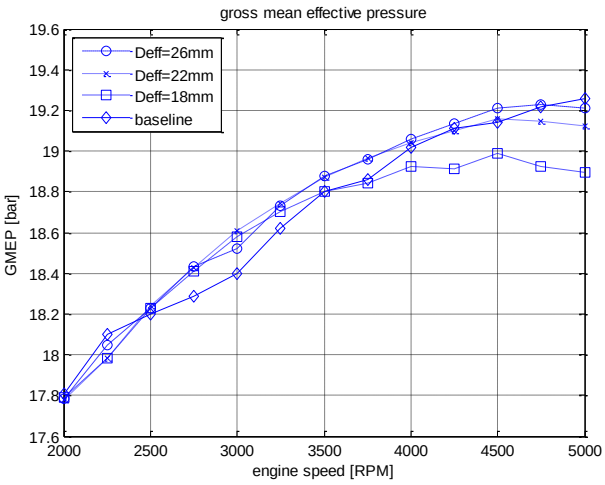

Figure 15 Gross indicated mean effective pressure

The ability of the TE engine models to shift the start of combustion angle toward the advance side by a couple of degrees (Figure 16) is not primarily due to the cooling effect, which, as explained earlier, is rendered practically ineffective as the charge enters the cylinder, but to an increase in the residual gas mass fraction. The total burn duration thus increases as the mode of combustion parameter (Figure 18) decreases, effectively allowing the

position of 50 % Mass Fraction Burnt (Figure 19) to be advanced by as much as 1 CAD approximately at the knock onset limit. As the GMEP data already shows, a slightly better efficiency is achieved.

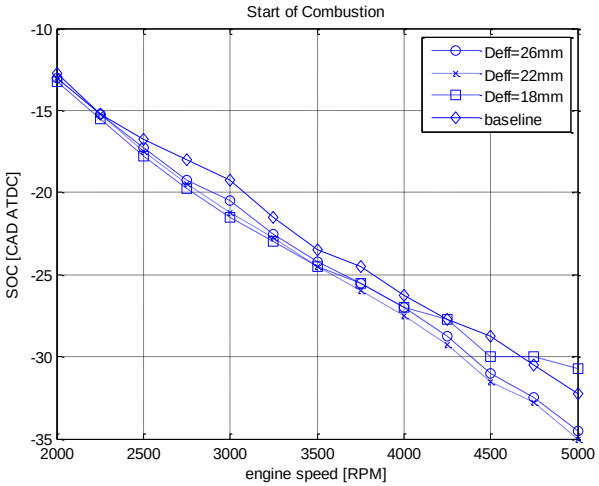

Figure 16 Spark angle

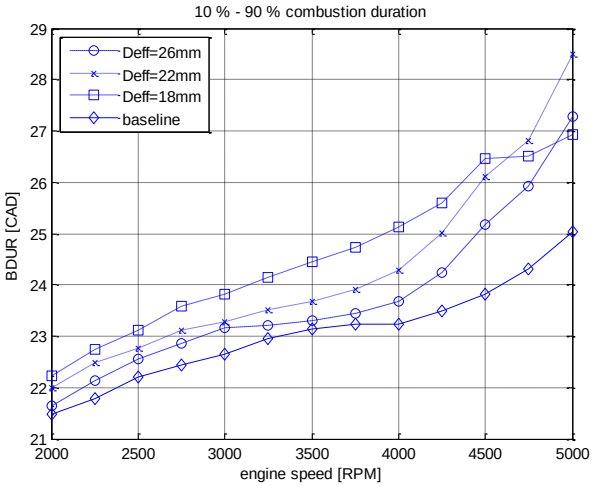

Figure 17 10 – 90 % mass fraction burnt duration

The effective parameters, taking also into account the power obtained from the turbo-expander, show promising values. Only the smallest turbocharger-equipped TE engine has a smaller BMEP (Figure 22) than the baseline engine, and only at engine speeds exceeding 3500 RPM. The highest values are associated with the medium (*Deff*=22 mm) and big exhaust turbine-equipped (*Deff*=26 mm) TE engine. As the volumetric efficiency is being regulated, the indicated and brake specific fuel consumption show trends that are reciprocal to their mean pressure counterparts.

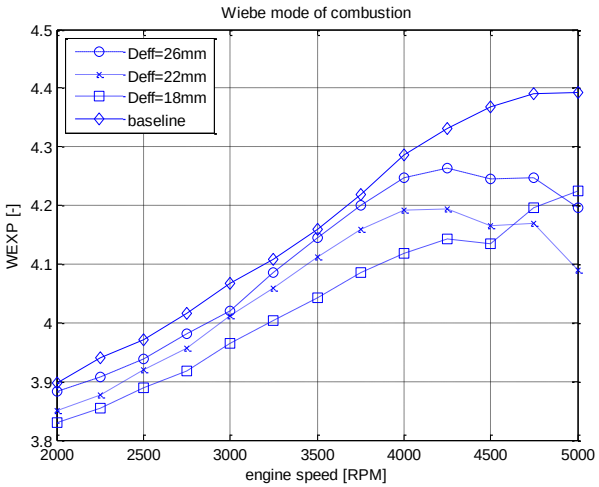

Figure 18 Wiebe mode of combustion parameter

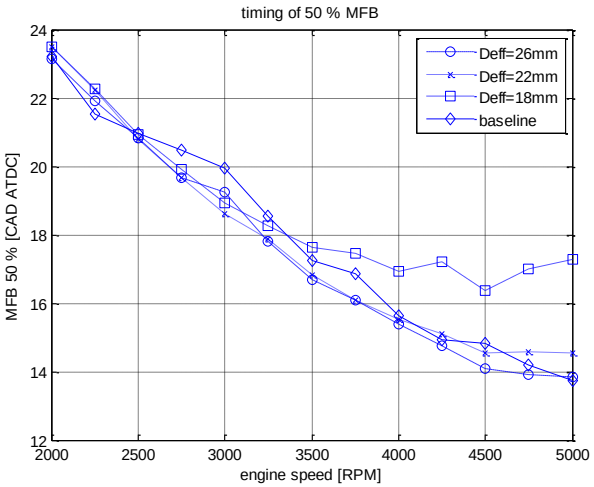

Figure 19 50 % MFB position

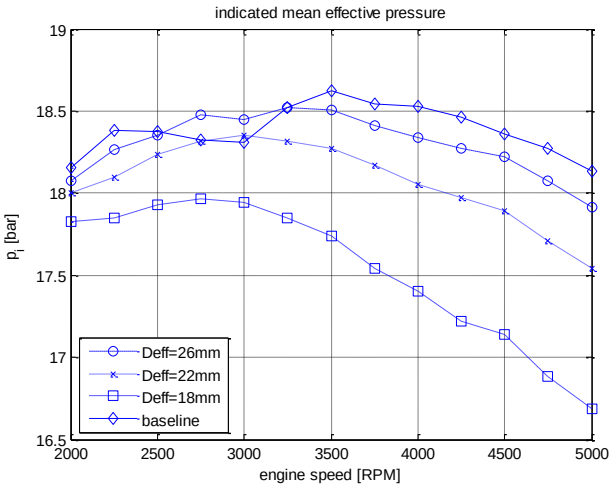

Figure 20 Indicated mean effective pressure

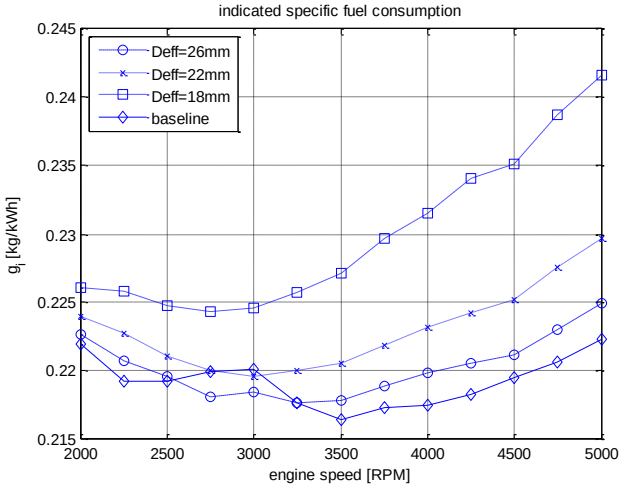

Figure 21 Indicated specific fuel consumption

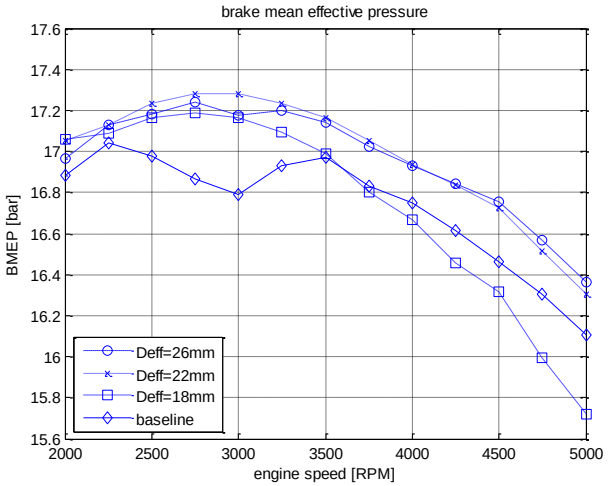

Figure 22 Brake mean effective pressure

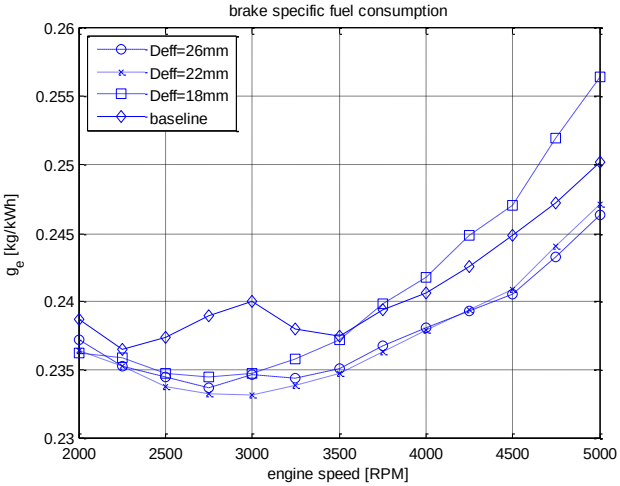

Figure 23 Brake specific fuel consumption

CONCLUSIONS

A simulation study regarding the potential benefits of a turbo-expansion system implementation on an SI engine has been conducted. In order to isolate the potential benefits of the system alone, a baseline engine incorporating a VTG turbocharger was conceived to serve as the basis for comparison. Indeed, had a wastegate-equipped turbocharger been implemented on the baseline engine, the benefits of the turbo-expansion system would have been greater because of increased backpressure caused by fractional exhaust flow use.

Even though a significant cooling effect is achieved in the intake system, it is greatly diminished when the fresh charge enters the cylinder in which an increased mass of residual gas is present. The indicated mean effective pressure comparison clearly shows that, aside from the engine speed range in which significant backflow occurs on the baseline engine model, the turbo-expander engine models produce less work in the cylinder for the same fresh charge mass. The primary cause is the increase in negative pumping work on the order of 0,25 bar in the best case (TE engine with *Deff*=26 mm).

However, the brake parameters show a certain advantage for the TE engine, primarily due to additional expansion power being transmitted to the crankshaft. Even then, the increase in efficiency is all but colossal, with maximum improvement in brake thermal efficiency of 1,8 percent at 4500 RPM. It should be noted that the conditions for achieving this brake efficiency gain are high isentropic efficiency of the turbines and the compressor, high intercooler effectiveness and effective use of the work available at the turbo-expander shaft. The latter represents probably the biggest challenge of all.

With regard to the turbo-expansion concept, future work should focus on investigating the potential benefits on different types of engines and different engine displacements. Additional efforts should be concentrated on optimal intake and exhaust cam phasing determination and full operating range simulations.

REFERENCES

[1] Atkins, K.A. and French, C.C.J.: "Thermal loading of a petrol engine", Proceedings of the Institution of Mechanical Engineers, 187, 1, 1973, 561-573,

[2] Douaud, A. M. and Eyzat, P.: "Four-Octane-Number Method for Predicting the Anti-Knock Behavior of Fuels and Engines", SAE Paper 780080, 1978,

[3] Lindström, F., Ångström, H., Kalghatgi, G. and Möller, C.: "An Empirical SI Combustion Model Using Laminar Burning Velocity Correlations," SAE Technical Paper 2005-01-2106, 2005,

[4] Ricardo WAVE 8.4 Help System,

[5] Taitt, D.W., Garner, C.P., Swain, E., Bassett, M.D., Pearson, R.J. and Turner, J.W.G.: "An automotive engine charge-air intake conditioner system: Thermodynamic analysis of performance characteristics", Proceedings of the Institution of Mechanical Engineers, Part D: Journal of Automobile Engineering, 219, 3, 2005, 389-404,

[6] Taitt, D.W., Garner, C.P., Swain, E., Blundell, D., Pearson, R.J. and Turner, J.W.G.: "An Automotive Engine Charge-Air Intake Conditioner System: Analysis of Fuel Economy Benefits in a Gasoline Engine Application", Proceedings of the Institution of Mechanical Engineers, Part D: Journal of Automobile Engineering, 220, 9, 2006, 1293-1307,

[7] Turner, J., Pearson, R., Bassett, M. and Oscarsson, J.: "Performance and Fuel Economy Enhancement of Pressure Charged SI Engines through Turboexpansion - An Initial Study," SAE Technical Paper 2003-01-0401, 2003.